Mie scattering from a sonoluminescing bubble with high spatial and temporal resolution

B. Gompf and R. Pecha
I. Physikalisches Institut, Universität Stuttgart, Pfaffenwaldring 57, D-70550 Stuttgart, Germany
(Received 4 August 1999; revised manuscript received 12 November 1999)

The dynamics of a single-air bubble trapped in a resonant sound field in water has been characterized by Mie scattering and a Streak camera with high spatial and temporal resolution. The streak images show that in the endphase of the cavitation collapse the scattered light intensity is no function of the bubble radius anymore. In the last nanoseconds around minimum bubble radius most of the light is scattered at the highly compressed water surrounding the bubble and not at the bubble wall. This leads to a minimum in the scattered light intensity about 700 ps before the sonoluminescence pulse is emitted. And neglecting this changes leads to a strong overestimation of the bubble-wall velocity. In the reexpansion phase the high spatial resolution of the streak camera allows one to distinguish between the light scattered at the bubble wall and the light scattered at the outgoing shock wave.

PACS number(s): 78.60.Mq, 43.25.+y

Single-air bubbles acoustically levitated in water can show extremely nonlinear oscillations leading to a very violent collapse and the emission of short light pulses [1]. The whole behavior of this remarkable phenomenon as the emitted broadband spectrum or the emission of pressure waves is strongly related to the bubble dynamics, i.e., how fast the bubble collapses [2,3]. In the past, several groups have shown that the bubble dynamics can be probed very accurately with Mie scattering [4,5]. Using large detection angles and assuming constant refractive indices during the whole bubble oscillation the scattered light intensity is approximately proportional to the square of the bubble radius. Radius-time curves measured in this way agree well with radius-time curves calculated with the Rayleigh-Plesset (RP) equation. On the other hand Holzfuss *et al.* discussed the possibility that at minimum bubble radius light is also scattered at the emitted shock wave and that this should be considered by the interpretation of scattered intensities [6].

In these earlier experiments the scattered light intensity was detected with photomultiplier tubes (PMT). The band width of PMT's limits the achievable time resolution than to about 5 ns. For comparison, the duration of the emitted light pulses is in the range of 100 ps [7,8]. On the other hand theoretical descriptions of the light emission in sonoluminescence need the exact behavior of bubble dynamics around minimum bubble radius on a time scale comparable to the duration of the emitted light pulses [9]. That is also true for predictions for upscaling sonoluminescence [10,11]. All these theories assume that the hydrodynamic models are valid on a ps time scale, which is not experimentally proofed until now. In Fig. 1, a comparison between radius-time curves measured with a PMT and calculated radius-time curves for three different driving pressures under otherwise equal conditions are shown. The calibration from intensity to radius was made under the above mentioned assumptions and for the calculation the RP equation as it is discussed in Ref. [12] was used. The increase of the equilibrium radius with increasing driving pressure is also considered. Whereas the expansion and the collapse phase on this time scale agree well, the afterbounces are not very good reproduced by the RP equation if the literature values for viscosity and surface tension are used. At minimum bubble radius the bubble seems to lose much more energy than predicted by the RP equation.

In this paper, we present streak camera measurements of the light scattered from a single bubble with sub-ns time resolution. Besides the high time resolution a streak camera has the advantage that it also allows a high spatial resolution in one direction. The experimental set-up is shown in Fig. 2. A single sonoluminescing (SL) bubble was trapped in a 250 ml spherical quartz glass flask filled with filtered, degassed water, which was driven at its first radial oscillation mode at 19 570 Hz by two piezoelectric disks. The resonator had two flat windows of high optical quality on opposite sides to enable undisturbed imaging of the bubble. The whole resonator is in a small cooling box (not shown in Fig. 2) to enable measurements at varies temperatures. At lower temperatures the space stability is much higher, an important condition for streak camera measurements. All results shown here were carried out at 6 °C. The gas concentration in the water was controlled with an oximeter and was in the range of 1 mg/l O_2, which corresponds to about 80 torr partial pressure [13]. The amplitude of the driving pressure P_a was measured by a polyvinylidene fluoride (PVDF) needle hydrophone, which was calibrated with a fiber optic probe hydrophone [14,15]. Light from a 20 mW HeNe laser was scattered at the bubble and than focused through one of the quartz windows onto the entrance slit of the Streak camera (Hamamatsu C5680 with fast single sweep unit M5676). The aperture of the system was limited by the quartz windows to about f/2.8. The angle between the optical axis of the streak camera and the laser was 25°. A red filter in front of the streak camera reduced the SL intensity to the level of the scattered light intensity. The streak camera was triggered by a fast PMT and a time delay on the previous SL pulse. Therefore the red laser light was blocked by an UV filter in front of this PMT. To increase the signal to noise ratio about 10^6 streak images were on-line integrated. Due to the high repetition rate of the camera this corresponds to a measuring time of only 1 min. In the 10–50 ns time windows used for our investigations, the time resolution was about 500 ps, limited mainly by the time jitter between subsequent SL pulses and not by the width of the entrance slit of the camera.

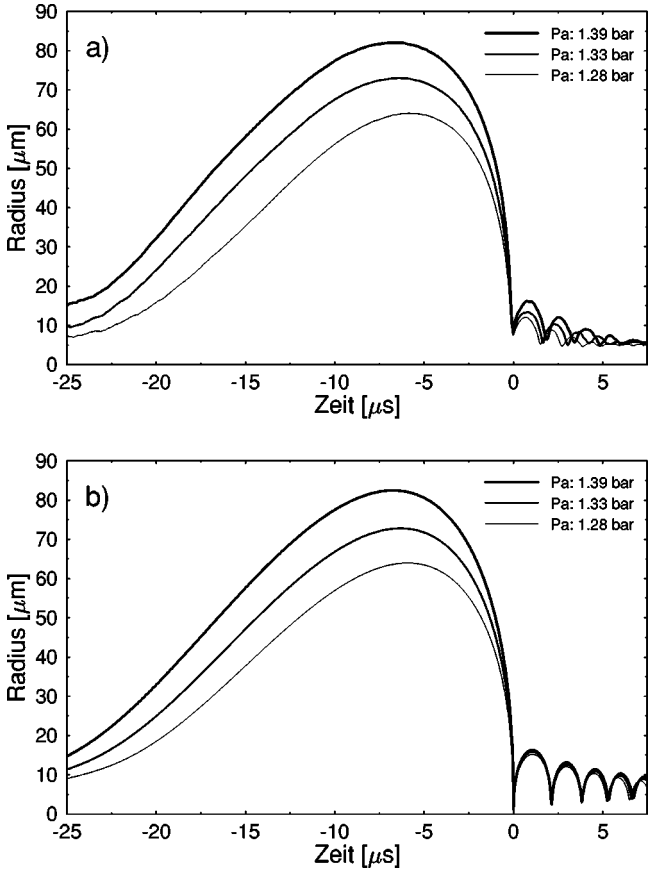

FIG. 1. Comparison between measured (a) and calculated (b) radius-time curves for three different driving pressures under otherwise equal conditions. Whereas the expansion and the collapse phase agree well at that time scale, the measured afterbounces are much smaller and their frequency is higher than predicted by the Rayleigh-Plesset equation.

In Fig. 3(a) a streak image of the collapse endphase on a 10-ns time window is shown. The time and space axis are marked by arrows, dark corresponds to high intensity. Therefore, the SL pulse itself appears as dark spot and is also marked. After the SL pulse one can distinguish three lines; the center line is caused by the reexpansion of the bubble, the two outer lines are caused by light scattered at the outgoing shock wave. In Fig. 3(b) two intensity profiles obtained from Fig. 3(a) are shown, one integrated along a selected area around the center line, one integrated over the whole streak image. Remarkable are the two pronounced minima in the scattered light intensity at -0.7 ns before and about 4.5 ns after the SL pulse especially in the center profile. They are due to Mie-lobe clusters and will be discussed below. The large difference between the two profiles indicates, that at the beginning of the reexpansion most of the light is scattered by the outgoing shock wave. The strongly nonlinear propagation of the launched shock wave which can clearly be seen in Fig. 3(a) is discussed by the authors in more detail in Ref. [16].

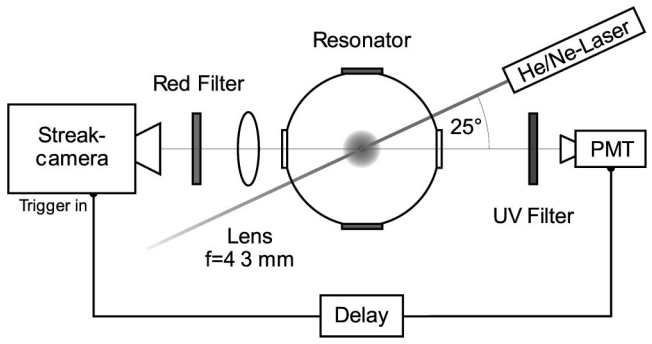

FIG. 2. Experimental setup. The laser light scattered at the oscillating bubble is detected with high spatial and temporal resolution by a streak camera. The streak camera is triggered by the previous SL pulse using a fast photomultiplier and a time delay.

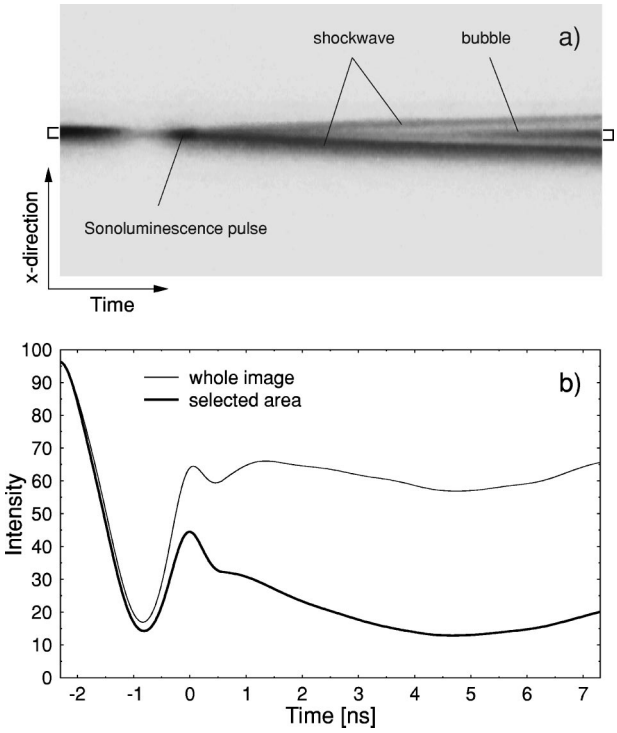

FIG. 3. (a) Streak image showing the last 10 ns of the bubble collapse. After the SL pulse three lines can be distinguished: the center line is due to light scattered at the bubble itself, the two outer lines correspond to the outgoing shock wave. (b) Intensity profiles integrated over the whole image and along a selected area around the center (marked by brackets).

In this paper, we will concentrate on the question, what one can learn about bubble dynamics from light scattering experiments. To translate the measured intensity versus time curve into a radius-time curve, which can be compared with theoretical models several assumptions have to be made. The bubble has to be spherical during the whole oscillation. This condition seems to be fulfilled, otherwise the streak image should not show only one spherical outgoing shock wave. And the refractive index profile, at which the light is scattered has to be known. For example some realistic profiles at minimum bubble radius are shown in Fig. 4. The bubble is surrounded by a sphere of highly compressed water and inside there will also be a more or less pronounced profile. How this profile looks like is not clear yet. In all former investigations either the scattered light intensity was assumed to be proportional to the square of the bubble radius [4,17], which totally neglects the complicated angular distribution of the Mie-scattering, or for the calculation of the

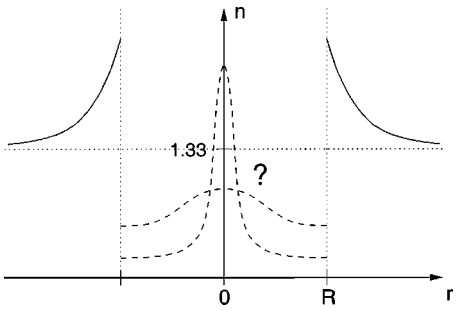

FIG. 4. Schematic drawing of the possible refractive index profiles inside and outside the bubble at minimum bubble radius (R: bubble wall). Solid line: Outside the bubble is shielded by a shell of highly compressed water with increased refractive index (refractive index under normal conditions: 1.33). Dashed lines: Inside the refractive index profile is not known but nearly all theoretical models consider a profile with a maximum in the center. There is no experimental evidence for an ingoing schockwave (steep center profile).

Mie-intensities a sphere was assumed with a refractive index of $n=1$ inside and $n=1.33$ outside [5]. To get an estimation which part of the index profile shown in Fig. 4 is most relevant for the scattered intensity we start with a very simple model: We calculated the expected Mie-intensities under the specific geometry of the experiment with the assumption of a pure argon bubble with equilibrium radius R_0 [18]. The refractive index inside the bubble was than calculated from the density using the Lorenz-Lorentz relationship. The increase of the refractive index in the surrounding water was neglected. Here we assumed that that part is separated by considering only the center profile of Fig. 3. In Fig. 5, the expected Mie-intensities received in this way are shown. Due to the limited aperture the scattered light intensity shows pronounced Mie-lobe clusters (LC). This LC's were used for absolute radius calibration in Fig. 6 [5]. One had to stress the fact, that when the wavelength of the used laser is comparable with the bubble radius, which is always the case at the endphase of the collapse, even the total scattered light intensity oscillates. At that time the assumption that the scattered light intensity is proportional to the square of the radius is not valid anymore for all geometries. Under the specific parameters of the experiment the RP equation gives a minimum radius of 0.8 μm, which in our simple model leads to a refractive index inside the bubble of $n=1.10$. For comparison Fig. 5 shows both curves, the expected Mie intensities with and without increasing refractive indices.

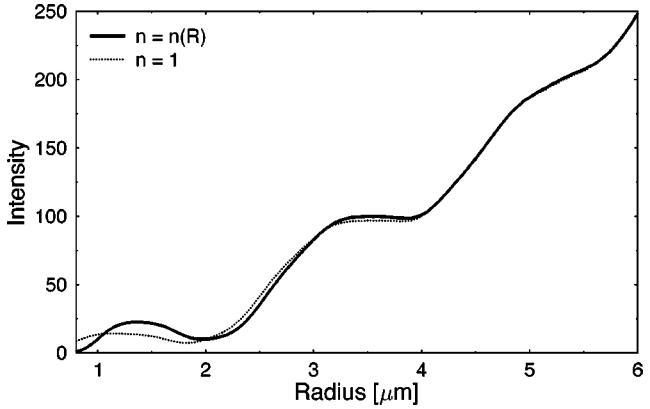

FIG. 5. Expected Mie-intensities versus radius calculated for the experimental geometry of Fig. 2 considering the increasing refractive index inside the bubble. For comparison the dashed line shows the situation for a refractive index of $n=1$.

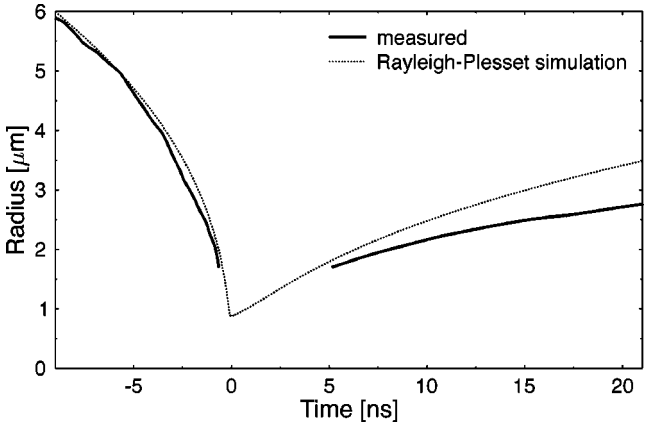

FIG. 6. Comparison between the measured radius-time curve obtained after calibration with a radius-time curve calculated from the Rayleigh-Plesset (RP) equation. The collapse phase down to about 1.7 μm is well described by the simulation, whereas the reexpansion is slower than predicted. In a time window of about 5 ns around minimum bubble radius most the light is scattered at the highly compressed water surrounding the bubble. In this region the intensity is much higher than the expected one shown in Fig. 5.

In a next step, we have translated our measured Mie-intensities (Fig. 3) with the expected Mie-intensities (Fig. 5) into a radius-time curve and compared it with a calculated radius-time curve obtained by the RP equation (Fig. 6). For the calculation only measured parameters obtained from the experiment ($P_a=1.28$ bar, $P_0=0.95$ bar, $R_0=5$ μm) and well known constants from literature ($c_w=1430$ m/s, $\sigma=0.075$ N/m, $\eta=0.0015$ Pa) had been used, so that there were no free fit parameters. The two minima in the scattered light intensity in Fig. 3 are due to the minimum at 2 μm in Fig. 5. Therefore, they disappear after radius calibration. In the collapse phase the agreement between simulation and experiment is good down to about 1.7 μm. In the region around the minimum the scattered light intensity is much higher than predicted by our simple model. As can be seen from Fig. 3 the minimum in the scattered light intensity is about 0.7 ns before the SL pulse. From this time on most of the light is scattered at the highly compressed water around the bubble leading to a strong increase in the scattered light intensity before minimum bubble radius. From Fig. 6 one get a bubble wall velocity 1 ns before the SL pulse of about 950 m/s. This value is much lower than the values found by Weninger, Barber, and Putterman [17]. They used a pulsed laser technique to probe the actual bubble size. And they assume a R^2 dependence of the scattered intensity neglecting any influence of Mie-lobe clusters and changes in refractive indices.

In the reexpansion phase, where the space resolution of the streak camera allows to separate the light scattered from the bubble itself from that scattered at the shock wave, the bubble wall velocity is much slower than predicted by the RP simulation. That means that the RP equation underestimates the energy loss at minimum bubble radius.

Whether the interior of the bubble is totally shielded by the compressed water or some of the light is still scattered at the center is not clear from our experiments. But in principle one can calculate Mie intensities also for complex pressure profiles as they are discussed in some single bubble sonoluminescence models [19,20].

In conclusion, our results show that in light scattering experiments especially in the collapse endphase the correct Mie intensities and the changes in refractive indices have to be considered. In the last 5 ns around minimum bubble radius most of the light is scattered by the developing shock wave. The space resolution of the streak camera allows to separate this part and to obtain radius-time curves down to about 1.7 μm, which can be compared with calculated radius-time curves without any free fit parameters. The bubble wall velocities obtained in this way are in good agreement with the RP equation but much lower than the values published by Weninger *et al.* [19].

The authors wish to thank W. Eisenmenger for stimulating discussions. We gratefully acknowledge financial support by the Bundesministerium für Forschung und Bildung.

[1] D. F. Gaitan, L. A. Crum, C. C. Church, and R. A. Roy, J. Acoust. Soc. Am. **91**, 3166 (1992).
[2] R. A. Hiller, K. R. Weninger, S. J. Putterman, and B. P. Barber, Science **266**, 248 (1994).
[3] Z. Q. Wang, R. Pecha, B. Gompf, and W. Eisenmenger, Phys. Rev. E **59**, 1777 (1999).
[4] B. P. Barber, R. A. Hiller, R. Löfstedt, S. J. Putterman, and K. R. Weninger, Phys. Rep. **281**, 65 (1997).
[5] W. J. Lentz, A. A. Atchley, and D. F. Gaitan, Appl. Opt. **34**, 2648 (1995).
[6] J. Holzfuss, M. Rüggeberg, and A. Billo, Phys. Rev. Lett. **81**, 5434 (1998).
[7] B. Gompf, R. Günther, G. Nick, R. Pecha, and W. Eisenmenger, Phys. Rev. Lett. **79**, 1405 (1997).
[8] R. Pecha, B. Gompf, G. Nick, Z. Q. Wang, and W. Eisenmenger, Phys. Rev. Lett. **81**, 717 (1998).
[9] S. Hilgenfeldt, S. Grossmann, and D. Lohse, Nature (London) **398**, 402 (1999).
[10] S. Hilgenfeldt and D. Lohse, Phys. Rev. Lett. **82**, 1036 (1999).
[11] J. Holzfuss, M. Rüggeberg, and R. Mettin, Phys. Rev. Lett. **81**, 1961 (1998).
[12] S. Hilgenfeldt, M. P. Brenner, S. Grossmann, and D. Lohse, J. Fluid Mech. **365**, 171 (1998).
[13] We prefer to give the measured gas concentration in the liquid, which is the relevant parameter for comparison with theory.
[14] J. Staudenraus and W. Eisenmenge, Ultrasonics **31**, 267 (1993).
[15] Z. Q. Wang, P. Lauxmann, C. Wurster, M. Köhler, B. Gompf, and W. Eisenmenger, J. Appl. Phys. **85**, 2514 (1999).
[16] R. Pecha and B. Gompf, Phys. Rev. Lett. **84**, 1328 (2000).
[17] K. R. Weninger, B. P. Barber, and S. J. Putterman, Phys. Rev. Lett. **78**, 1799 (1997).
[18] For the calculation the program Mietab 6.38 by A. Miller was used.
[19] W. C. Moss, D. B. Clarke, and D. A. Young, Science **276**, 1398 (1997).
[20] Vi Q. Vuong and A. J. Szeri, Phys. Fluids **8**, 2354 (1996).